Available online at www.sciencedirect.com

ScienceDirect

Procedia CIRP 71 (2018) 460–465

www.elsevier.com/locate/procedia

4th CIRP Conference on Surface Integrity (CSI 2018)

Effect of cutting speed on the surface integrity of face milled 7050-T7451 aluminium workpieces

I. Perez[a], A. Madariaga[a]*, M. Cuesta[a], A. Garay[a], P.J. Arrazola[a], J.J Ruiz[b], F.J. Rubio[b],R. Sanchez[b]

[a]*Mondragon Uniberstitatea, Faculty of Engineering, Loramendi 4, Arrasate-Mondragón, 20500, Spain*
[b]*Aerometallic (Aernnova Group), Pol. Industrial Tarazona, 50500, Spain*

* Corresponding author. Tel.: +34 943 71 22 74; fax: +34 943 71 19 21. E-mail address: amadariaga@mondragon.edu

Abstract

The guarantee of surface integrity has become a primary objective for researchers when analysing the reliability of machined aircraft aluminium alloy structural parts in high-speed machining. This work studies the effect of cutting speed on the surface integrity of face milled 7050-T7451 aluminium workpieces. First, 7050-T7451 aluminium workpieces were face milled under dry conditions using three cutting speeds (200, 800, 1400 m/min) at constant feed (0.20 mm/tooth) and depth of cut (1 mm). An indexable face milling cutter with a diameter of 50 mm with five uncoated inserts was used in the face milling tests. During the machining process, cutting forces were acquired employing a Kistler dynamometer in order to understand the influence of the mechanical load on the final surface quality. The surface roughness produced by the milling process was measured using a portable rugosimeter. The residual stresses generated by the cutting process were measured by the hole-drilling technique. In addition, small specimens were cut out from the workpieces and microstructural alterations of the surface layer were analysed employing optical microscopy techniques. The results demonstrate that the magnitude of residual stresses and the thickness of the affected layer is sensitive to the cutting speed, while surface roughness and microstructural defects do not show significant variations for the tested conditions.

Selection and peer-review under responsibility of the scientific committee of the 4th CIRP Conference on Surface Integrity (CSI 2018).

Keywords: alumimium alloys; milling; surface integrity

1. Introduction

The demand for fuel-efficient and lightweight aircraft has promoted the use of large aluminium thin-walled monolithic parts due to their high specific strength, low cost and good forming properties.

High-speed machining is the main process to manufacture large aluminium parts. Furthermore, during the manufacturing of these monolithic parts, a high amount of material is removed by machining processes, up to 90% [1].

The durability of the airframe is also one of the key factors in the design of aeroplanes [2]. With the high-level concern on working reliability of machined aircraft aluminium alloy structural parts in high-speed machining (HSM), the guarantee of surface integrity (surface roughness, residual stress, micro-hardness and microstructure defects) becomes primary objective for researchers to accomplish [3]. Surface integrity has a major importance on in-service failures such as corrosion and fatigue life of the parts, and properties of surface integrity like residual stresses can also significantly affect part distortions [4]. Therefore, it is essential to define the machining conditions that induce an appropriate surface integrity to prevent from early in-service failures and reduce costs on surface works.

Many researchers have investigated the effect of machining parameters on the surface integrity of nickel-based alloys, titanium alloys, or high strength steels [5-7]. However, in the literature, there were few studies found which focused on surface integrity produced by machining processes in aircraft aluminium alloy structural parts.

Selection and peer-review under responsibility of the scientific committee of the 4th CIRP Conference on Surface Integrity (CSI 2018).
10.1016/j.procir.2018.05.034

Ammula and Guo [8], based on a Design of Experiments (DOE) method, analysed the surface integrity generated by milling in 7050-T7451 and 6061-T651 aluminium alloys. For the tested conditions, they found that cutting speed had a dominant effect on average surface roughness, increasing the roughness as the cutting speed increased. By contrast, Zhong *et al*. [9] found lower values of surface roughness when increasing the cutting speed in high-speed machining tests of 7050-T7451 aluminium alloy. They also observed that, even though the surface roughness was low, surfaces machined at 5000 m/min suffered from gradual deterioration, due to chip adherence and metal smearing.

Denkena *et al.* [10] studied the influence of cutting conditions and tool geometry on the residual stresses (RS) generated during milling of forged aluminium 7449-T7651. They found that an increase of cutting speed and feed led to more compressive residual stresses, and also a reduction of the cutting edge radius produced more compressive residual stresses. Masoudi *et al.* [11] analysed the effect of cutting speed, feed and insert material on the residual stresses induced by turning in 7075-T6 aluminium alloy. They observed that a decrease in cutting speed or an increase in feed rate produced more compressive residual stresses as a consequence of higher cutting forces. Huang *et al.* [12] also found that increasing cutting speed or reducing the feed rate generated a less compressive residual stress on the machined surface in 7050-T7451 aluminium alloy. Jeelani and Biswas [13] performed orthogonal cutting tests in 2024-T351 aluminium and they concluded that the rake angle had a minimum effect on the residual stress, while a more compressive stress profile was generated when increasing the cutting speed.

The literature review has revealed contradictory conclusions, in particular regarding the effect of cutting speed on surface roughness and residual stresses generated when machining aluminium alloys. This work is aimed at understanding the effect of cutting speed on surface integrity produced when machining 7050-T7451 aluminium alloy. For that purpose, face milling tests were carried out, machining forces were measured during the tests and the surface integrity (microstructural alterations, surface roughness and residual stresses) of the machined specimens was assessed.

2. Materials and experiments

2.1. Material

The specimen for machining tests was extracted by water jet assisted machining from a 100 mm thick 7050-T7451 aluminium rolled plate. The dimensions of this specimen were 100 mm long, 112 mm wide and 40 mm high. The longitudinal direction of this specimen was perpendicular to the rolling direction of the plate. The selected material had a yield stress of 470 MPa, a rupture stress of 574 MPa and a Young's modulus of 71 GPa.

2.2. Milling experiment

The specimen was fixed to a triaxial sensor Kistler dynamometer (9129AA) in order to measure machining forces in three orthogonal directions during the tests.

Fig. 1 shows schematically the machined specimen. First, the specimen was face milled at roughing conditions but using a different number of machining passes. This produced steps in the workpiece that allowed identification of the surfaces machined under different cutting conditions in the subsequent tests. Then, the finishing up-milling operations were carried out at three different cutting conditions, while the feed rate, depth of cut and width of cut were kept constant. The conditions used in the tests are summarised in Table 1. It should be noted that three finishing passes were performed in each surface to increase reliability of the measurements of machining forces.

An indexable face milling cutter with a diameter of 50 mm with five uncoated inserts (APKT L93 1604PDFR) was used in the face milling tests. The properties of the inserts are shown in Table 2.

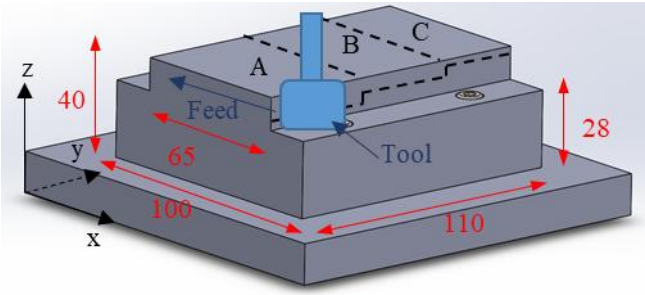

Fig. 1. Scheme of the face milling tests and dimensions of the specimen. Dimensions in mm.

Table 1. Cutting conditions.

Test	Cutting speed [m/min]	Feed rate [mm/tooth]	Depth of cut [mm]	Width of cut [mm]
A	200	0.20	1	37.5
B	800	0.20	1	37.5
C	1200	0.20	1	37.5

Table 2. Properties of the APKT L93 1604PDFR uncoated inserts.

Material	Rake angle [°]	Clearance angle [°]	Nose radius [mm]	Edge radius [µm]
Uncoated WC-Co	11	8	0.2	12-18

3. Surface Integrity characterisation

The surface integrity of the three tested conditions was characterised: microstructural defects, surface roughness and residual stresses. To ensure that these measurements were performed at the same points of the three machined surfaces, a reference line was set. This reference line was aligned with

the centre of the tool and parallel to the feed direction, as depicted in Fig. 2.

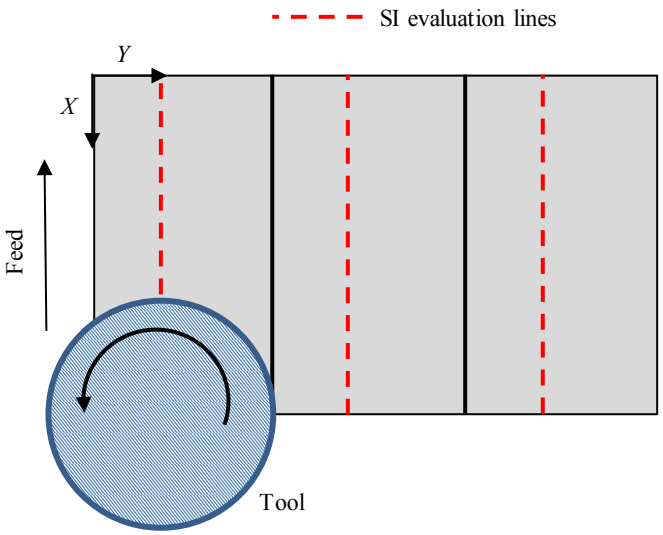

Fig. 2. Top view of the machined specimen showing the lines where surface integrity was evaluated.

3.1. Microstructural observation

The specimens for microstructural observations were cut out from the surfaces machined at three different cutting conditions. The microstructure was analysed in two directions: in the transverse direction (close to cutting direction) and in the longitudinal (feed direction). These specimens were hot mounted in a phenolic resin with carbon filler, ground employing Silicon Carbide papers and polished to obtain the desired surface quality. Then, the specimens were chemically etched using Keller's reagent. The microstructure of the specimens was observed in a Leica DM IRM optical microscope.

3.2. Surface roughness

A portable Mitutoyo SJ-210 rugosimeter was used to measure average surface roughness R_a, the total height of the roughness profile R_t and the mean roughness depth R_z on the three machined surfaces. The measurements were carried out using the UNE-EN ISO 4288:1998 Standard. The parameters used in the measurements are the following: 2 µm stylus tip radius, filtering of the measured profile with a cut-off wavelength λ_s=2.5 µm and filtering of the primary profile with the cut-off wavelength λ_c=0.8 mm, and evaluation length of 5 times λ_c.

3.3. Residual Stresses

The machining-induced residual stresses were measured at the centre and end of each of the machined surfaces, in order to avoid inlet and outlet effect of the tool. Machining-induced residual stresses were measured using the hole-drilling technique and following the ASTM-E837-13 standard. As residual stresses generated by machining processes are located in a very shallow layer, fine increments were used, following the recommendations given by Grant *et al.* [14].

First, Vishay Measurement Group target strain gauges EA-06-031RE-120 were bonded in the centreline of the tool path (reference line shown in Fig. 2). The hole-drilling tests were performed employing a Restan MTS3000 machine, using a high-speed air turbine and drill bits of 0.8 mm diameter. The incremental hole-drilling procedure was carried out at each strain gauge employing a total of 16 depth increments. The first five increments had a depth of 10 µm, the next four increments had a depth of 20 µm, and the final seven increments a depth of 50 µm. This sequence of increments produced a hole with a diameter of ≈0.95 mm and a depth of 500 µm. Strains were recorded in a HBM data acquisition system after each increment. Finally, the residual stress profiles were calculated by the procedure given in the ASTM-E837-13.

4. Results and discussion

4.1. Milling forces

The cutting forces were measured using the Kistler dynamometer. From the Kistler dynamometer forces were obtained in the three directions identified in Fig.1: F_x (feed direction), F_y (transverse direction) and F_z (thrust direction). The magnitude of forces varied significantly during the beginning and final step of each machining pass. Therefore, the stable zone of machining forces was considered for this analysis, as can be seen in the example of Fig. 3.

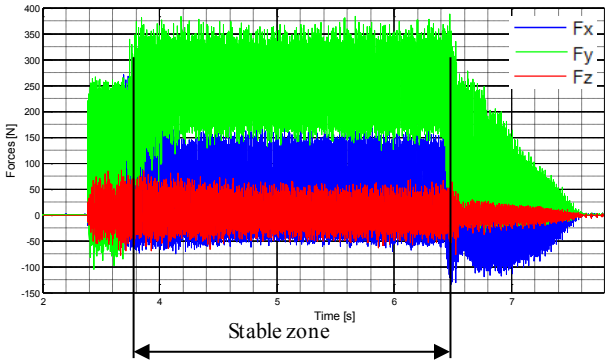

Fig. 3. Machining forces vs time during machining trials and identification of the stable zone, at 200 m/min cutting speed.

As explained in section 2.2. machining forces were measured three times for each cutting condition. Fig. 4 shows the maximum forces and Fig. 5 shows the absolute value of average forces in each direction.

As expected, machining forces were higher in the *X* (feed direction) and the *Y* direction (transverse direction) compared to the *Z* direction, where very low values were measured. When increasing the cutting speed from 200 m/min to 800 m/min maximum forces decreased, possibly due to the softening of the removed material or reduction of chip thickness. However, when machining at 1400 m/min cutting speed, maximum forces decreased in the *X* direction, but increased in the *Y* direction. Likely, this increase in the maximum cutting force F_y and its amplitude, were associated

with a dynamic instability of the tool or fixture system in the *Y* direction at high cutting speeds. However, as can be seen in Fig. 5, the average value of the machining forces in the *Y* direction was also reduced when increasing the cutting speed: 256 N at 200 m/min, 210 N at 800 m/min and 182 at 1400 m/min.

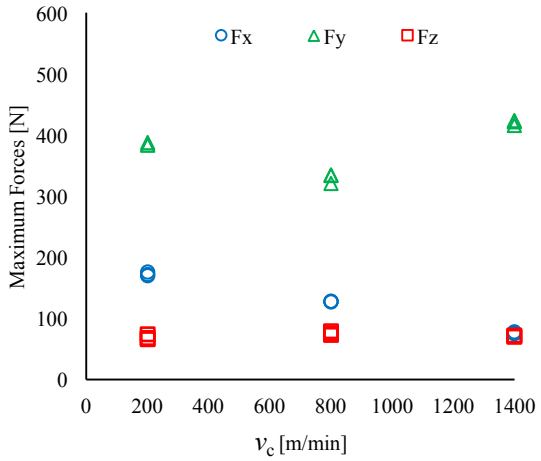

Fig. 4. Maximum machining forces vs cutting speed.

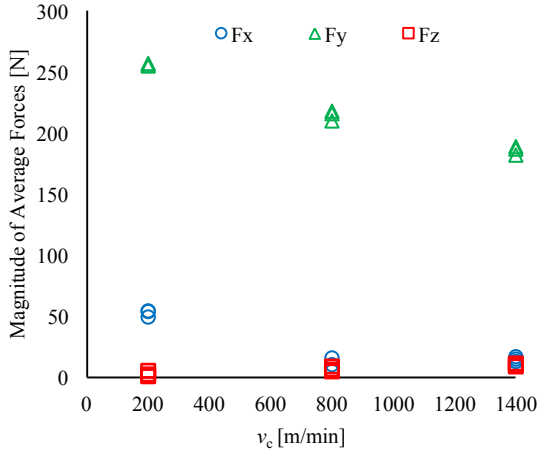

Fig. 5. Absolute value of average forces vs cutting speed.

4.2. Microstructure defects

The main defects observed in the analysed specimens were: surface drag, heavily distorted layer and steps.

Surface drag, which consists of oriented grains with respect to the microstructure of the base material, fundamentally in the cutting direction, was the predominant subsurface defect. In general, surface drag was found together with a heavily distorted layer, which can be identified as a heavy deformation of the surface layer microstructure. The presence of the last one was more evident in the feed direction. These defects and their magnitude were similar in specimens obtained from the surfaces machined at the three cutting conditions, with an average affected depth of ≈ 10 µm and a maximum of ≈ 17 µm (Fig. 6).

The most common surface defect were steps, or irregular surface (Fig. 7) which predominantly were found in the cutting direction. The magnitude of the defects was similar in the three machined surfaces, with an average height of ≈ 6 µm and a maximum of ≈ 9 µm.

Based on the criteria of the aeronautical industry, it can be summarised that the surface layer affected by the machining conditions is acceptable (lower than 17 µm) and the three cutting conditions studied in this paper can be considered as gentle.

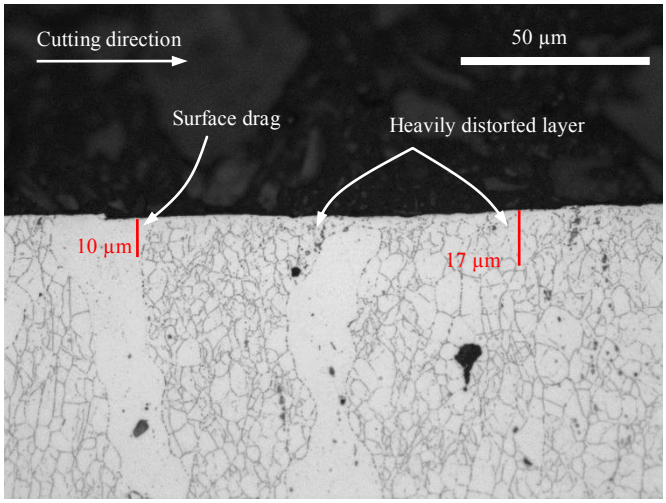

Fig. 6. Example of surface drag and heavily distorted layer.

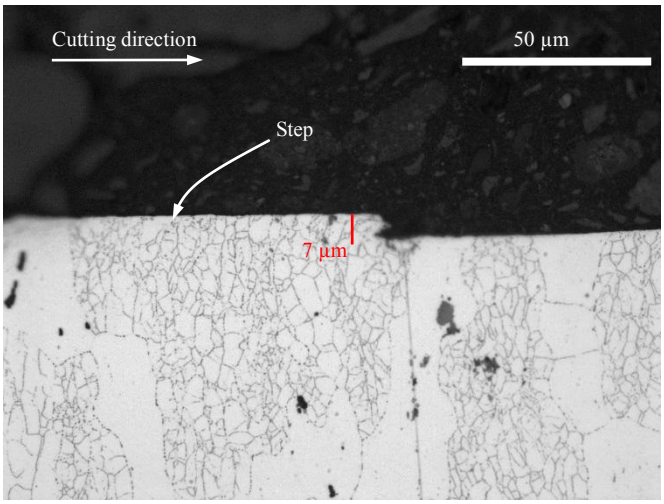

Fig. 7. Example of a step found at the machined surface.

4.3. Surface roughness

Table 3 compares the results of average surface roughness R_a, the total height of the roughness profile R_t and the mean roughness depth R_z of the three machined surfaces. As can be seen in Table 2, the three tested conditions led to similar surface roughness values, $R_a \approx 1.4$ µm, $R_t \approx 7.6$ µm and $R_z \approx 6.5$. Although some authors have reported that surface roughness varies considerably in aluminum alloys when modifying the cutting speed [8, 9], in this study conditions R_a, R_z and R_t showed similar values for the tested conditions. Theoretically, surface roughness mainly depends on the feed and tool geometry, and those parameters were identical in the three milling tests.

Table 3. Surface roughness measurements.

Cutting speed [m/min]	R_a [µm]	R_t [µm]	R_z [µm]
200	1.35±0.25	7.48±1.53	6.23±1.33
800	1.41±0.27	7.98±0.27	6.55±0.67
1200	1.52±0.29	7.88±1.45	6.83±1.35

4.4. Residual Stresses

Fig. 8 and Fig. 9 show the residual stress profiles in the cutting and feed direction respectively. As it can be seen, residual stress profiles were different at the lowest cutting speed (200 m/min) compared to the two highest cutting speed (800-1400 m/min).

At a cutting speed of 200 m/min, an initial tensile residual stress of 70 MPa is generated at the surface in the cutting direction, which then becomes compressive at a depth of 30 µm, reaching a maximum compressive stress of ≈-100 MPa at a depth of 100 µm, and finally residual stresses are stabilised at a depth of 200-250 µm. The residual stress profile was similar in the feed direction, but a higher maximum compressive residual stress was found (≈-150 MPa).

By contrast, compressive residual stresses were generated at the surface, in both cutting and feed directions when machining at higher cutting speeds. It should be noted that the shape of the residual stress profile obtained in each direction was different. In the cutting direction, the maximum compressive residual stress was induced at the surface (≈-200 MPa), and the compressive layer reached a depth of 200-250 µm. The compressive layer was thinner when milling at the highest cutting speed. In the feed direction, although compressive residual stresses were generated at the surface, a compressive residual stress peak of ≈-160 MPa was found at a depth of 30 µm. Then, compressive residual stresses were stabilised at a depth of 200 µm.

As it is well known, the thermal loads generated during machining produce more tensile residual stresses while mechanical loads lead to compressive residual stresses. Therefore, at the lowest cutting speed the thermal effect was dominant, generating non-desirable tensile residual stresses at the surface in the cutting direction. However, when the cutting speed was increased, as a consequence of a higher mechanical effect (also higher heat dissipation ratio through the chip) a compressive residual stress layer was generated in both cutting and feed direction.

For the tested conditions, it cannot be found a clear relationship between measured machining forces and residual stresses. As expected, the highest machining forces were developed at the lowest cutting speed, but this cutting condition did not generated higher magnitude of compressive residual stresses. However, a thicker compressive residual stress layer was developed, mainly in the feed direction, which could be due to the higher cutting forces (F_x and F_y). In addition, when machining at a cutting speed of 800 m/min slightly more compressive residual stresses and a slightly thicker compressive residual stress layer was generated. In fact, machining forces (maximum and average value) were slightly higher (≈10%) at 800/min cutting speed. This last observation suggests that possibly at high speed machining conditions there is a good agreement between cutting forces and machining-induced residual stresses.

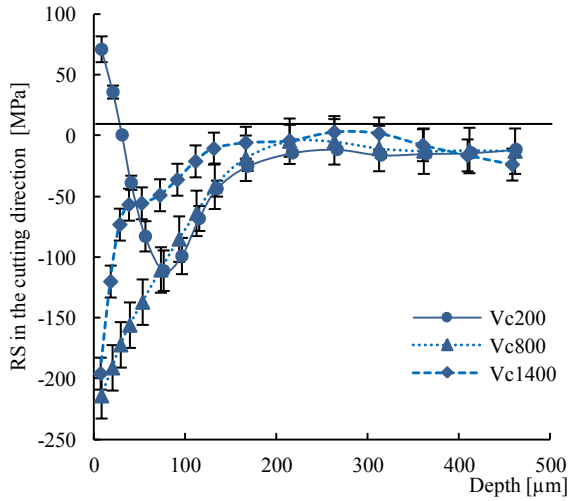

Fig. 8. Residual stress profiles in the cutting direction.

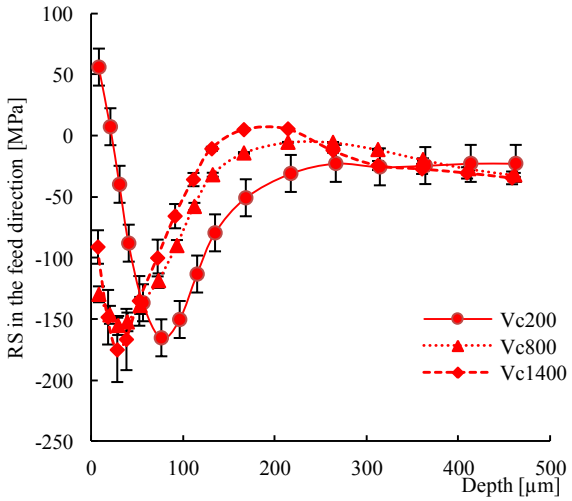

Fig. 9. Residual stress profiles in the feed direction.

5. Conclusions

The main conclusions of this work are the following:

- Machining forces decreased when increasing the cutting speed.
- The main subsurface defects were surface drag and presence of heavily distorted layer, and the maximum defect did not exceed 17 µm in depth. The most frequent surface defect was the formation of steps. The presence of surface drag, a heavily distorted layer and steps did not show a dependence on the cutting speed for the studied range of cutting conditions.
- Surface roughness did not vary significantly when modifying the cutting speed for the tested conditions.
- Tensile surface residual stresses were generated at the lowest cutting speed due to a higher thermal effect. A compressive residual stress layer was generated at higher cutting speeds. These compressive residual stresses (peak

value and affected thickness) were higher at 800 m/min cutting speed due to higher machining forces.

- Based on the results of this study, machining at 800 m/min cutting speed would be recommend as it produces beneficial compressive residual stresses while surface roughness and defects are similar to the two other cutting conditions.

Acknowledgements

The authors thank the Spanish Governments for the financial support given to the project TEMPROCEN (CIEN_IDI-20141299).

References

[1] Li JG, Wang SQ. Distortion caused by residual stresses in machining aeronautical aluminum alloy parts: recent advances. Int J Adv Manuf Technol 2017; 89(1):997-1012.

[2] Campbell Jr, FC. Manufacturing technology for aerospace structural materials. 1st ed. Elsevier; 2006.

[3] Yao CF, Dou X, Wu D, Zhou Z, Zhang J. Surface integrity and fatigue analysis of shot-peening for 7055 aluminum alloy under different high-speed milling conditions. Adv Mech Eng 2016; 8(10):1687814016674628.

[4] Madariaga A, Perez I, Arrazola PJ, Sanchez R, Ruiz JJ, Rubio FJ. Reduction of distortions in large aluminium parts by controlling machining-induced residual stresses Int J. Adv Manuf Technol 2018, https://doi.org/10.1007/s00170-018-1965-2.

[5] Jawahir IS, Brinksmeier E, M'saoubi R, Aspinwall DK, Outeiro JC, Meyer D, Umbrello D, and Jayal AD. Surface integrity in material removal processes: Recent advances. CIRP Ann-Manuf Technol 2011, 60(2):603-626.

[6] Ulutan D, Ozel T. Machining induced surface integrity in titanium and nickel alloys: A review. Int J Mach Tool Manu 2011; 51(3):250-280.

[7] Thakur A, Gangopadhyay S. State-of-the-art in surface integrity in machining of nickel-based super alloys. Int J Mach Tool Manu 2016; 100: 25-54.

[8] Ammula SC, Guo YB. Surface integrity of Al 7050-T7451 and Al 6061-T651 induced by high speed milling. SAE Technical Paper, 2005.

[9] Zhong Z, Ai X, Liu Z, Liu J, Xu Q. Surface morphology and microcrack formation for 7050-T7451 aluminum alloy in high speed milling. Int J. Adv Manuf Technol 2015; 78(1):281-296.

[10] Denkena B, Boehnke D, De Leon L. Machining induced residual stress in structural aluminum parts. Prod Engineer 2008; 2(3):247-253.

[11] Masoudi S, Amini S, Saeidi E, Eslami-Chalander H. Effect of machining-induced residual stress on the distortion of thin-walled parts. Int J Adv Manuf Technol 2015; 76(1-4):597-608.

[12] Huang X, Sun J, Li J, Han X, Xiong Q. An experimental investigation of residual stresses in high-speed end milling 7050-T7451 aluminum alloy. Adv Mech Eng 2013: 5:592659.

[13] Jeelani S, Biswas S, Natarajan R. Effect of cutting speed and tool rake angle on residual stress distribution in machining 2024-T351 aluminium alloy—unlubricated conditions. J Mater Sci 1986; 21(8):2705-2710.

[14] Grant P, Lord J, Whitehead P, Fry AT. The application of fine increment hole drilling for measuring machining-induced residual stresses. Appl Mech Mater Trans Tech Publications 2005; 105-110.